

Electronic Supplementary Information

Sensitive imaging of tumor using a nitroreductase-activated fluorescence probe in the NIR-II window

Xiaofan Zhang,^{ab} Xiaohua Li,^{*ab} Wen Shi^{ab} and Huimin Ma^{*ab}

^a Beijing National Laboratory for Molecular Sciences, Key Laboratory of Analytical Chemistry for Living Biosystems, Institute of Chemistry, Chinese Academy of Sciences, Beijing 100190, China

^b University of Chinese Academy of Sciences, Beijing 100049, China

E-mail: lixh@iccas.ac.cn, mahm@iccas.ac.cn

Contents

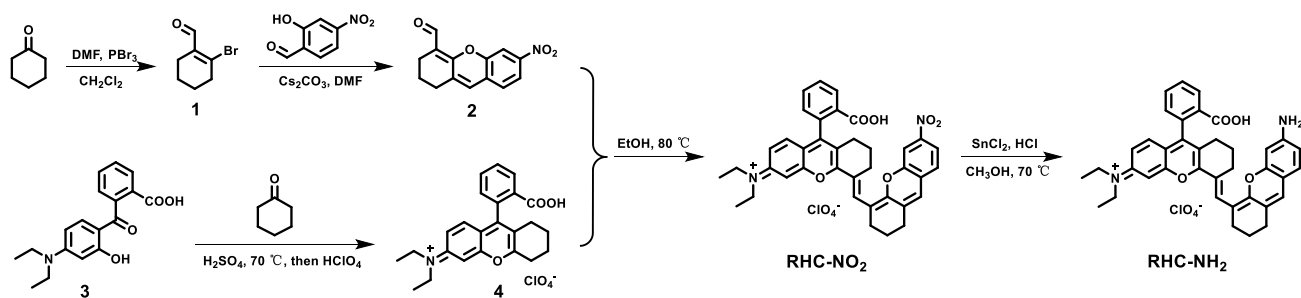
- 1. Apparatus and reagents**
- 2. Syntheses and characterizations**
- 3. General procedure for NTR detection**
- 4. Calculation of fluorescence quantum yield**
- 5. Determination of detection limit**
- 6. Cell culture and cytotoxicity assay**
- 7. In vivo imaging of mice**
- 8. Additional tables and figures**
- 9. References**

1. Apparatus and reagents

¹H NMR and ¹³C NMR spectra were obtained on Bruker Fourier 300 or 400 spectrometer. Electrospray ionization mass spectra (ESI-MS) were measured with a LC-MS 2010A instrument (Shimadzu, Japan). High-resolution electrospray ionization mass spectra (HR-ESI-MS) were acquired on an APEX IV FTMS instrument (Bruker, Daltonics). UV-vis absorption spectra were recorded on a UV-2600 (Shimadzu) spectrometer with an integrating-sphere accessory in 1-cm quartz cell. Fluorescence spectra were measured on NIRQuest-512 spectrophotometer (Ocean Optics) in 1×1 cm quartz cell. High-performance liquid chromatography (HPLC) assays were performed on LC-20AT and SPD-20A (Shimadzu) with Ultimate XB-C18 column (5 μm, 4.6 mm×250 mm, Welch Materials, Inc.). The absorbance measurements for MTT analysis were measured on a SpectraMax i3 microplate reader (Molecular Devices, USA). *In vivo* fluorescence imaging was carried out with the In Vivo NIR-II imaging system (In Vivo Master, Wuhan Grand-imaging Technology Co., LTD) equipped with InGaAs camera C-RED2 (Firstlight). The images were obtained with excitation at 808 nm and the emissions were collected with a 1000-nm longpass filter (Edmund Optics, Barrington, New Jersey). The excitation intensity of 808 nm laser was 80 mW/cm², and the exposure time was indicated in the corresponding figure legends.

Cyclohexanone, tin (II) chloride, cesium carbonate and β-nicotinamide adenine dinucleotide, reduced disodium salt hydrate (NADH) were obtained from InnoChem Science & Technology Co. Ltd. 2-Hydroxy-4-nitrobenzaldehyde and dicoumarin were obtained from TCI Co. 2-(4-(Diethylamino)-2-hydroxybenzoyl) benzoic acid and phosphorus tribromide were purchased from J & K Scientific Ltd. Nitroreductase from *Escherichia coli* and 3-(4,5-dimethyl-2-thiazolyl)-2,5-diphenyl-2*H*-tetrazolium bromide (MTT) were obtained from Sigma-Aldrich. All the cell lines used, Dulbecco's modified Eagle's medium (DMEM) and Roswell Park Memorial Institute (RPMI) 1640 were purchased from KeyGEN BioTECH Co. Ltd., Nanjing, China. Fetal bovine serum (FBS) was obtained from Invitrogen Corporation. Ultrapure water (over 18 MΩ·cm) was made by a Milli-Q reference system (Millipore). The stock solution of NTR was prepared with ultrapure water and stored in small aliquots at -20 °C to avoid repeated freeze-thaw cycles. The stock solution (1 mM) of the probe was prepared with DMSO.

2. Syntheses and characterizations



Scheme S1. Syntheses of RHC-NO₂ and RHC-NH₂.

Synthesis of compound 1: PBr₃ (24.8 mL) was added dropwise to the mixture of DMF (22.4 mL) and CH₂Cl₂ (100 mL) at 0 °C. After 45 min, cyclohexanone (10 mL) was added and the mixture was stirred overnight at room temperature under N₂ atmosphere. Then the resulting solution was poured into ice and NaHCO₃ was added slowly until pH = 7. After standing for some time, the aqueous layer was collected and extracted with CH₂Cl₂ (200 mL). The combined organic layer was dried over anhydrous Na₂SO₄. The filtrate was then concentrated under reduced pressure to provide an orange oil **1** (15.5 g), which was used directly in the next step.

Synthesis of compound 2: Compound **1** (1.36 g) was dissolved in DMF (20 mL), then 2-hydroxy-4-nitrobenzaldehyde (1 g) and Cs₂CO₃ (5.85 g) were added to the solution. The solution was stirred overnight at room temperature under N₂ atmosphere. The insoluble substances were then filtered and the filtrate was concentrated. The resulting residue was dissolved in CH₂Cl₂ (100 mL) and washed with saline (3 × 100 mL). The organic layer was dried over anhydrous Na₂SO₄, filtered and concentrated under reduced pressure. The crude product was purified by column chromatography on silica gel using ethyl acetate/petroleum ether (1/6, v/v) as the eluent to afford compound **2** as an orange solid (0.92 g, yield: 60%). ¹H NMR (400 MHz, 298 K, DMSO-d₆; Fig. S1): δ 10.31 (s, 1H), 8.04 (d, J = 1.6 Hz, 1H), 7.97 (dd, J = 2.4, 8.4 Hz, 1H), 7.57 (d, J = 8.4 Hz, 1H), 7.09 (s, 1H), 2.62 (t, J = 5.6 Hz, 2H), 2.30 (t, J = 5.6 Hz, 2H), 1.62-1.68 (m, 2H). ¹³C NMR (100 MHz, 298 K, DMSO-d₆; Fig. S2): δ 188.1, 158.7, 151.5, 147.8, 134.2, 128.2, 127.4, 125.3, 119.4, 114.9, 111.0, 29.8, 21.5, 20.0. HR-ESI-MS (Fig. S3), calcd for C₁₄H₁₁NNaO₄ [M+Na]⁺: *m/z* 280.05858; found: *m/z* 280.05773.

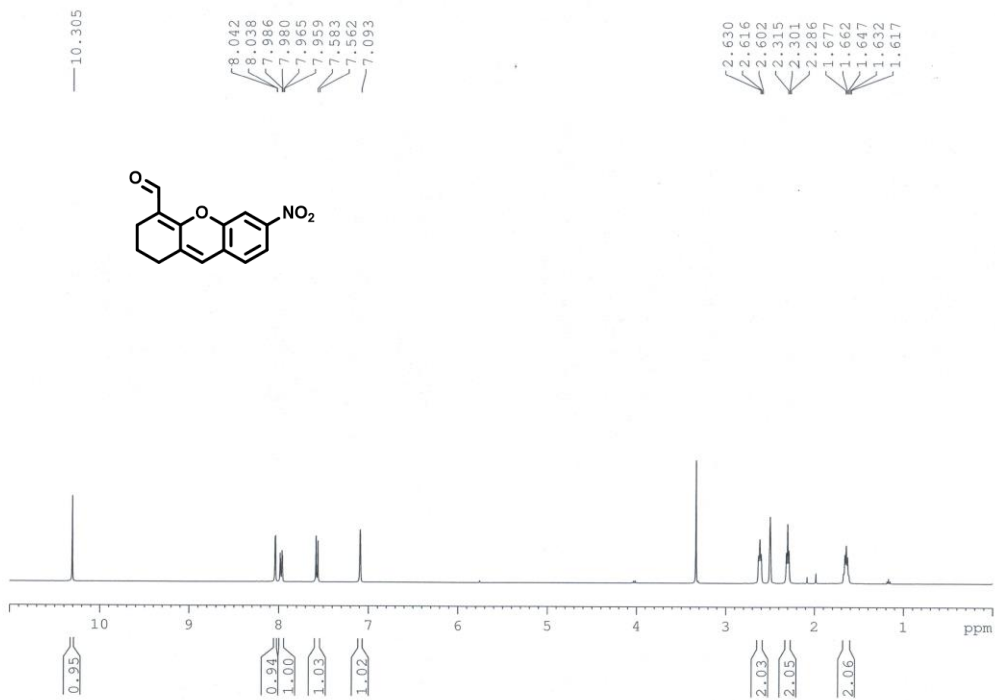


Fig. S1 ¹H NMR spectrum of **2** (400 MHz, 298 K, DMSO-d₆).

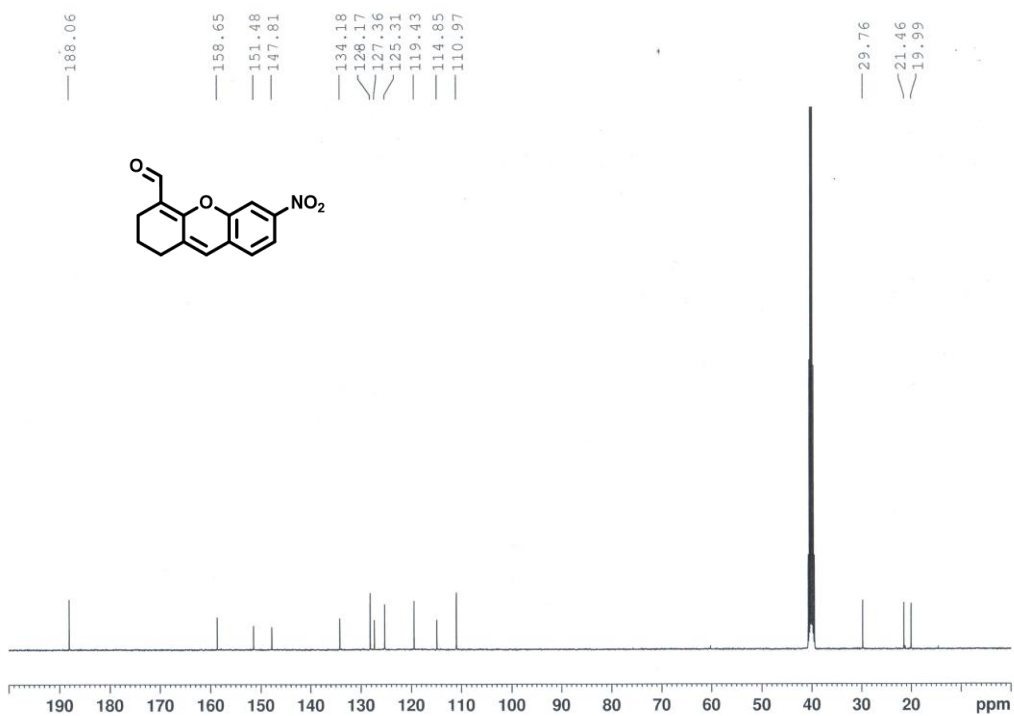


Fig. S2 ¹³C NMR spectrum of **2** (100 MHz, 298 K, DMSO-d₆).

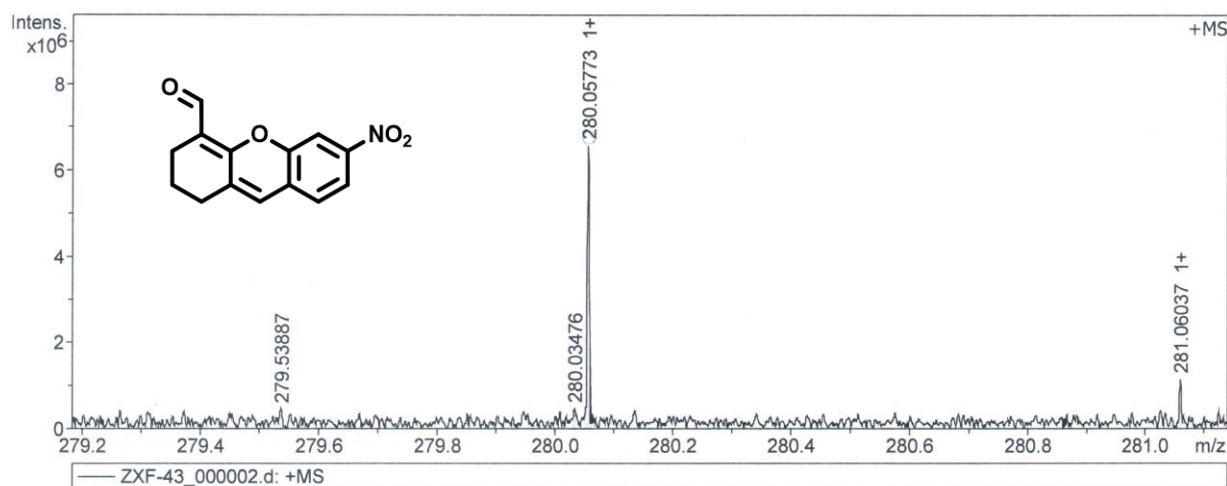


Fig. S3 HR-ESI-MS of **2**.

Synthesis of compound 4: Compound **4** was synthesized according to the previous literature.¹

Synthesis of probe RHC-NO₂: Compound **2** (257 mg) and **4** (524 mg) were dissolved in EtOH (20 mL). The mixture was then refluxed at 80 °C for 6 h under N₂ atmosphere. After cooling to room temperature, the solvent was removed by evaporation under reduced pressure. The residue was subjected to the silica gel chromatography with the eluent of CH₂Cl₂/CH₃OH (100/1 to 50/1, v/v), affording probe RHC-NO₂ as a black solid (683 mg, yield: 95%). ¹H NMR (300 MHz, 298 K, DMSO-d₆; Fig. S4): δ 8.17 (d, J = 7.5 Hz, 2H), 7.94 (d, J = 8.7 Hz, 2H), 7.87 (t, J = 7.5 Hz, 1H), 7.76 (t, J = 7.5 Hz, 1H), 7.49 (d, J = 8.4 Hz, 1H), 7.38 (d, J = 7.5 Hz, 1H), 7.00-7.32 (br, 2H), 6.78-6.99 (br, 2H), 3.56-3.73 (m, 4H), 2.70-2.92 (m, 4H), 2.58-2.69 (br, 2H), 2.06-2.30 (br, 2H), 1.60-1.84 (m, 4H), 1.18-1.32 (m, 6H). ¹³C NMR (75 MHz, 298 K, DMSO-d₆; Fig. S5): δ 167.2, 161.2, 157.4, 154.7, 152.4, 152.3, 147.3, 136.0, 135.4, 133.8, 131.7, 131.0, 130.7, 129.9, 129.7, 129.1, 128.7, 127.5, 126.5, 123.2, 121.5, 119.5, 117.3, 116.1, 115.9, 110.5, 95.8, 45.7, 29.7, 28.2, 27.3, 25.8, 21.7, 21.4, 12.8. HR-ESI-MS (Fig. S6), calcd for C₃₈H₃₅N₂O₆ [M]⁺: m/z 615.24896; found: m/z 615.24940.

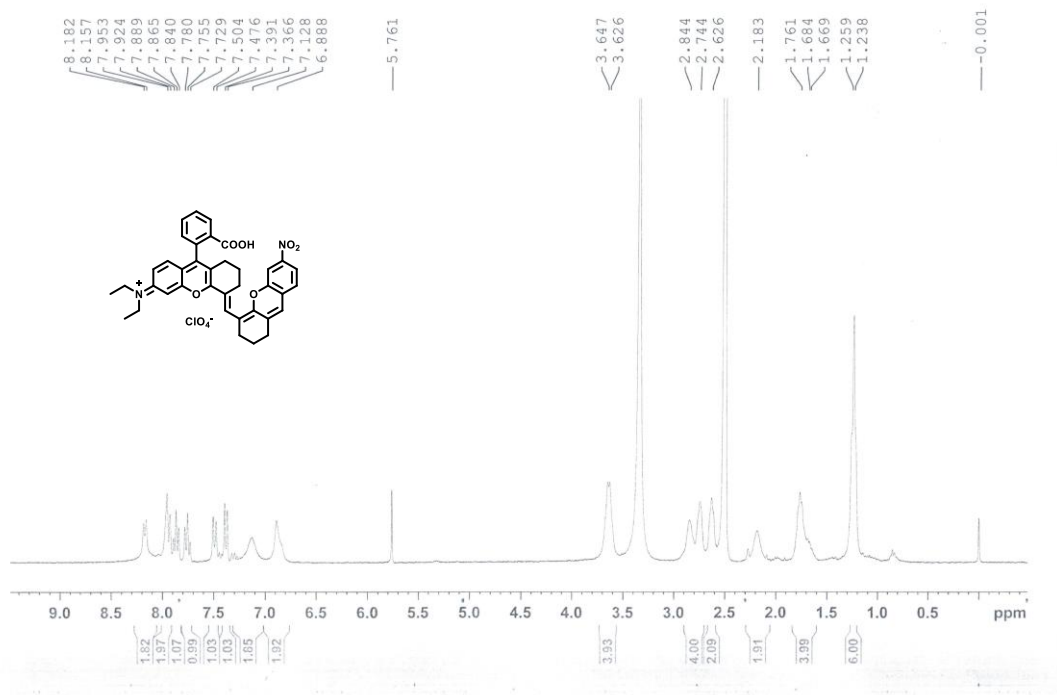


Fig. S4 ¹H NMR spectrum of RHC-NO₂ (300 MHz, 298 K, DMSO-d₆).

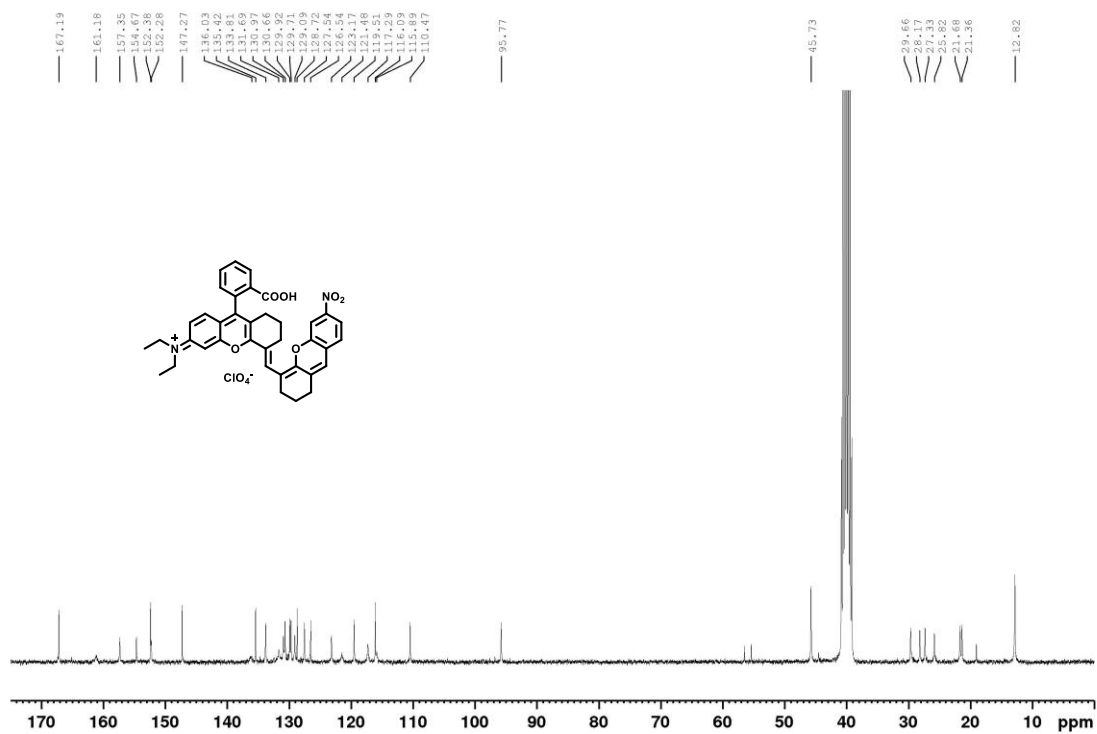


Fig. S5 ¹³C NMR spectrum of RHC-NO₂ (75 MHz, 298 K, DMSO-d₆).

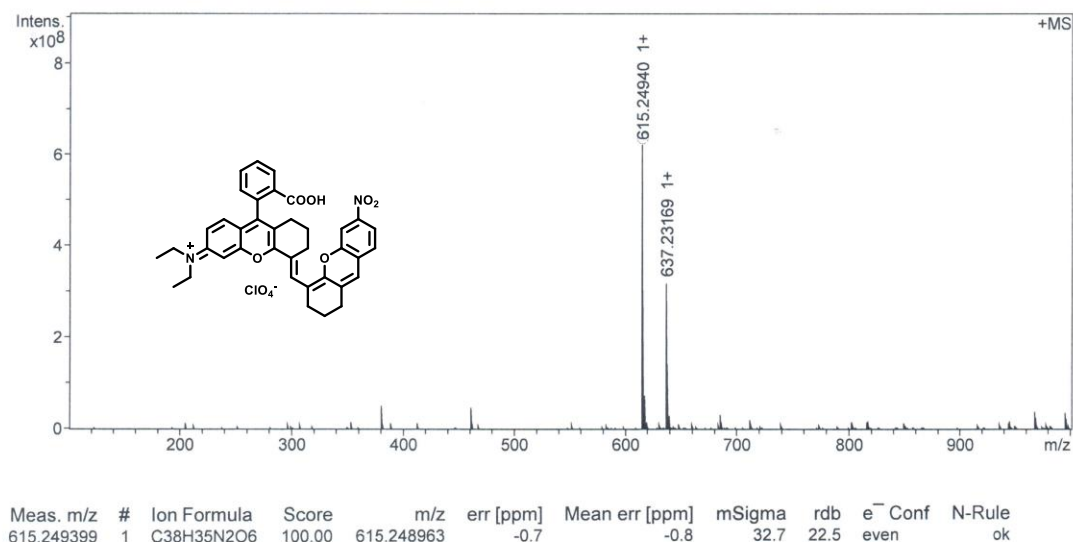


Fig. S6 HR-ESI-MS of RHC-NO₂.

Synthesis of RHC-NH₂: Probe RHC-NO₂ (251 mg) and SnCl₂ (1.33 g) were first dissolved in CH₃OH (20 mL). Then concentrated hydrochloric acid (1.5 mL) was added slowly to the above mixture under N₂ atmosphere. The reaction solution was refluxed at 70 °C for 5 h. After cooling to room temperature, the solution was neutralized by saturated Na₂CO₃, and the precipitate was filtered and washed with CH₂Cl₂ (5 mL). The collected filtrate was washed with H₂O (3 × 50 mL) and dried over anhydrous Na₂SO₄. The solvent was evaporated under reduced pressure, and the residue was subjected to the silica gel chromatography with the eluent of CH₂Cl₂/CH₃OH (50/1 to 10/1, v/v), affording RHC-NH₂ as a brown solid (120 mg, yield: 50%). ¹H NMR (400 MHz, 298 K, DMSO-d₆; Fig. S7): δ 7.93 (d, J = 7.6 Hz, 1H), 7.78 (t, J = 7.6 Hz, 1H), 7.66 (t, J = 7.6 Hz, 1H), 7.33 (d, J = 7.6 Hz, 1H), 7.06 (s, 1H), 6.79 (d, J = 8.0 Hz, 1H), 6.45 (d, J = 9.2 Hz, 2H), 6.38 (d, J = 8.4 Hz, 1H), 6.27 (s, 1H), 6.19 (d, J = 7.6 Hz, 2H), 5.43 (s, 2H), 3.36-3.42 (m, 4H), 2.53-2.62 (m, 1H), 2.38-2.46 (m, 4H), 1.79-1.88 (m, 1H), 1.64-1.72 (m, 2H), 1.48-1.62 (m, 4H), 1.10 (t, J = 6.8 Hz, 6H). ¹³C NMR (100 MHz, 298 K, DMSO-d₆; Fig. S8): δ 169.4, 154.2, 152.4, 151.4, 150.7, 149.6, 148.5, 148.0, 135.5, 130.2, 128.7, 127.7, 127.2, 126.7, 125.3, 124.6, 124.4, 124.0, 121.6, 111.2, 109.5, 109.3, 108.7, 106.6, 105.4, 105.3, 99.6, 97.0, 44.3, 29.9, 29.8, 28.6, 23.5, 22.6, 22.1, 12.8. HR-ESI-MS (Fig. S9), calcd for C₃₈H₃₇N₂O₄ [M]⁺: m/z 585.27478; found: m/z 585.27485.

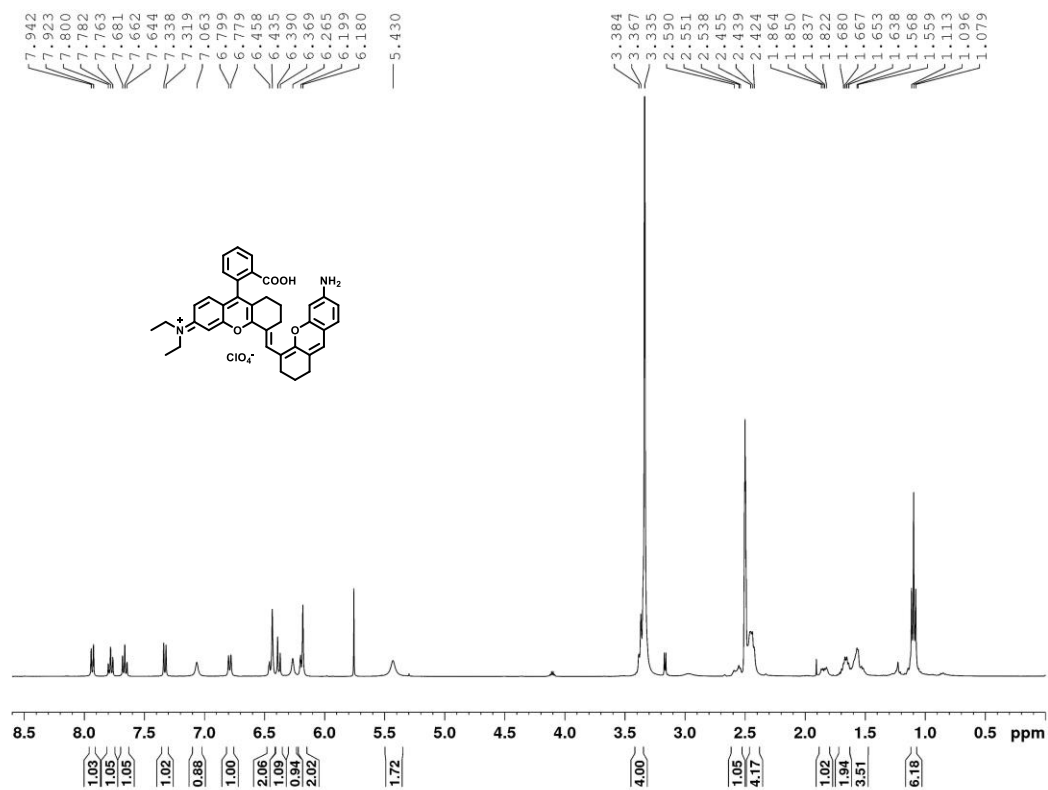


Fig. S7 ¹H NMR spectrum of RHC-NH₂ (400 MHz, 298 K, DMSO-d₆).

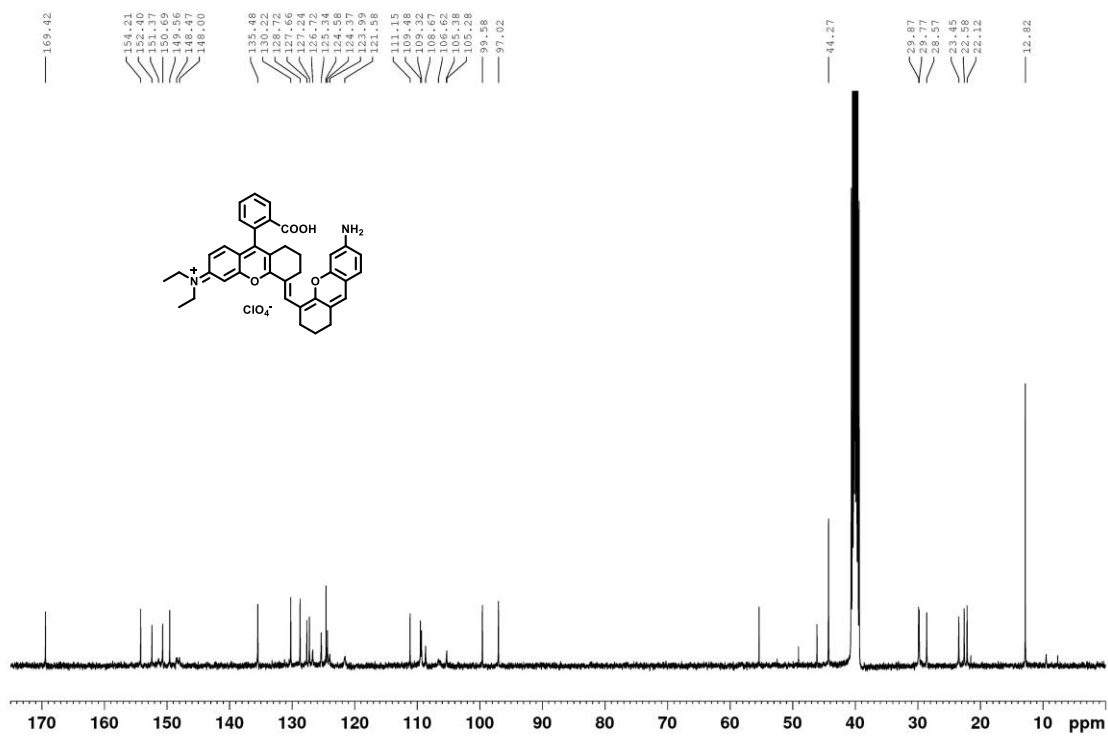


Fig. S8 ¹³C NMR spectrum of RHC-NH₂ (100 MHz, 298 K, DMSO-d₆).

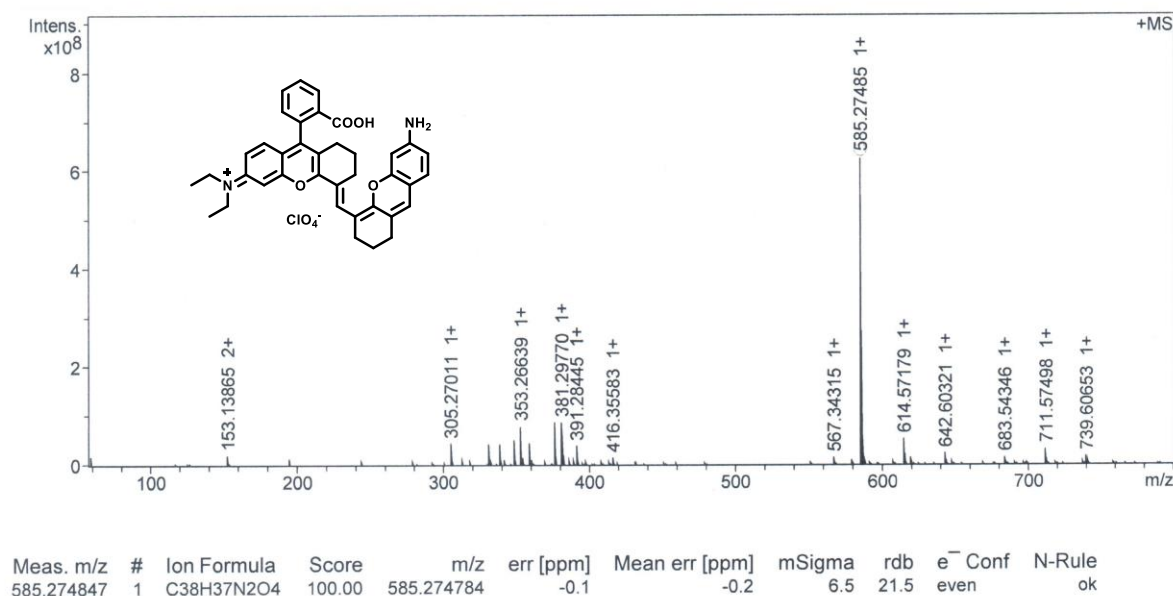


Fig. S9 HR-ESI-MS of RHC-NH₂.

3. General procedure for NTR detection

Unless otherwise stated, all the measurements were made in 20 mM pH 7.4 phosphate buffer containing 10% volume fraction of FBS (referred to as PBS) according to the following procedure. In a test tube, 4 mL of PBS and 50 μ L of probe RHC-NO₂ (1 mM) were mixed, followed by addition of an appropriate volume of NTR or other substances. The final volume was adjusted to 5 mL with PBS, and the reaction solution was mixed rapidly (note: for all tests about NTR, a final concentration of 200 μ M NADH was used). After incubation at 37 $^{\circ}$ C for 1 h in a thermostat, a 3 mL portion of the reaction solution was transferred to a quartz cell of 1 cm optical length to measure the absorbance or fluorescence with 808 nm laser excitation. In the meantime, a blank solution containing no NTR (control) was prepared and measured under the same conditions for comparison.

4. Calculation of fluorescence quantum yield

Fluorescence quantum yield (Φ) was measured in a similar method described previously.² Briefly, Φ was measured using optically matching solutions of IR26 ($\Phi = 0.05\%$ in dichloroethane) as a reference,³ and was calculated using the following equation:

$$\Phi_s = \Phi_r (A_r F_s / A_s F_r) (n_s^2 / n_r^2)$$

where the subscripts s and r denote sample and reference, respectively; A is the absorbance, F is the integrated fluorescence intensity, and n is the refractive index of the solvent. In this work, the excitation wavelength is at 808 nm while keeping the absorbance below 0.05.

5. Determination of detection limit

The detection limit (DL) was determined based on the following formula:

$$DL = 3SD/\text{slope}$$

where SD is the standard deviation of eleven blank measurements ($n = 11$), and the slope is the slope of the linear curve from fluorescence titration, as shown in Fig. 2B in the main text.

6. Cell culture and cytotoxicity assay

A549 cells were cultured in RPMI 1640 supplemented with 10% (v/v) FBS and 1% (v/v) penicillin-streptomycin at 37 °C in a humidified 5% CO₂ incubator. HeLa cells were cultured in DMEM with 10% (v/v) FBS and 1% (v/v) penicillin-streptomycin in a similar manner. The cytotoxicity of the probe to cells was evaluated using MTT assay as described previously.⁴

7. In vivo imaging of mice

Five-week-old female BALB/c nude mice were purchased from Beijing Vital River Laboratory Animal Technology Co., Ltd. All animal experimental procedures were performed in accordance with the Animal Management Rules of the Ministry of Health of the People's Republic of China and were approved by the Institute of Process Engineering, Chinese Academy of Sciences. A549 tumor-bearing mice were obtained by injection of 1×10^6 A549 cells suspended in PBS on the right shoulder of each mouse. HeLa tumor-bearing mice were obtained by injection of 1×10^6 HeLa cells suspended in PBS on the left shoulder of each mouse. After two weeks, tumor-bearing mice were used in our experiments.

8. Additional tables and figures

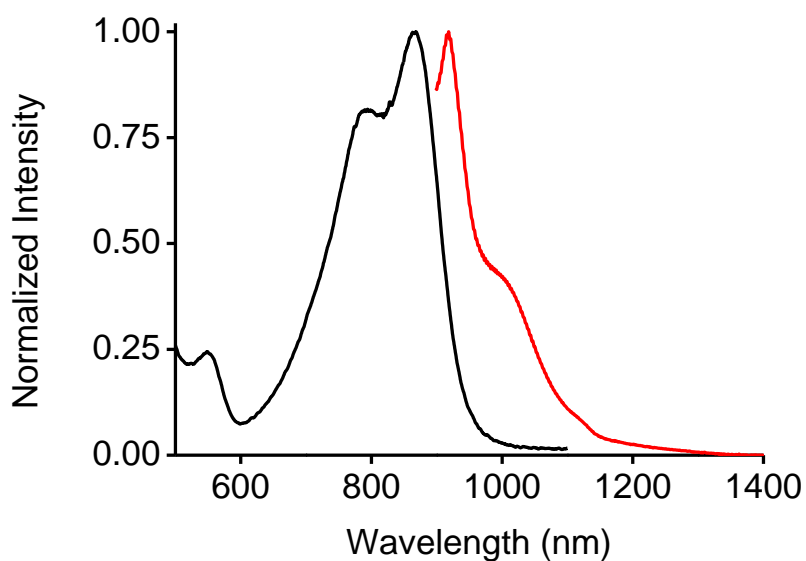


Fig. S10 The normalized absorption (black) and emission spectra (red) of RHC-NH₂ (10 μM) in PBS (pH 7.4, containing 10% FBS).

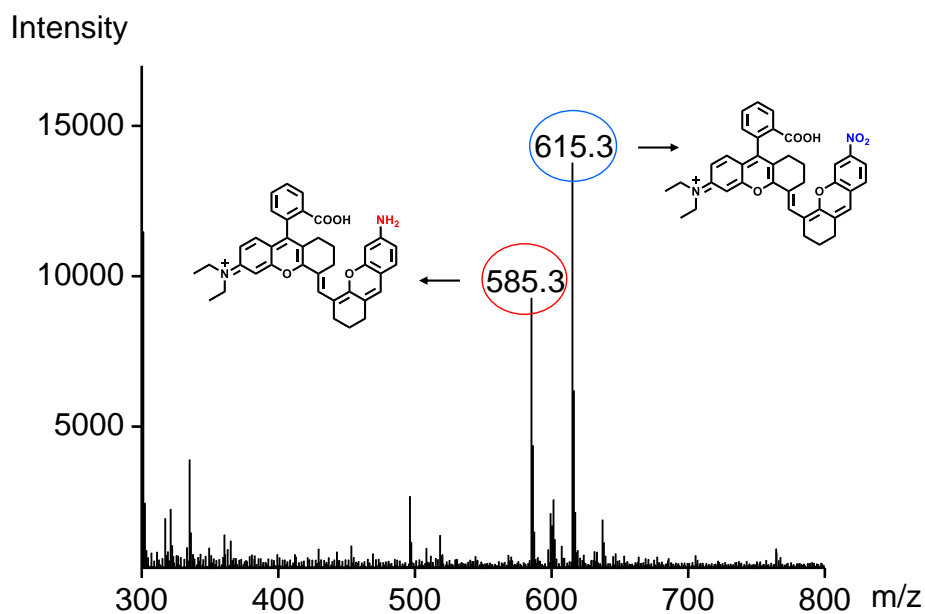


Fig. S11 ESI mass spectrum of the reaction solution of probe RHC-NO₂ (50 μM) with NTR (20 μg/mL). The peak at m/z = 585.3 reflects the generation of RHC-NH₂; the peak at m/z = 615.3 is the remaining RHC-NO₂.

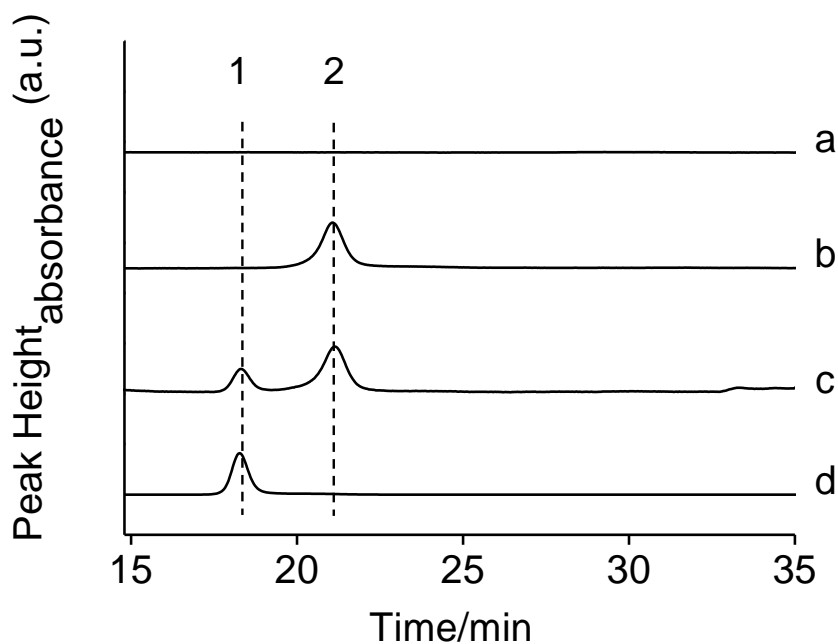


Fig. S12 Chromatograms of different reaction systems. (a): control, NTR (20 $\mu\text{g/mL}$) and NADH (1 mM); (b): probe RHC-NO₂ (50 μM); (c): probe RHC-NO₂ (50 μM) and NTR (20 $\mu\text{g/mL}$) in the presence of NADH (1 mM); (d): the reaction product RHC-NH₂ (50 μM). Assignments of the peaks: (1) 18.3 min, RHC-NH₂; (2) 21.1 min, probe RHC-NO₂. HPLC conditions are as follows: methanol/water (with 0.1% TEA) = 75/25 (v/v); flow rate = 0.3 mL/min; detection wavelength = 760 nm.

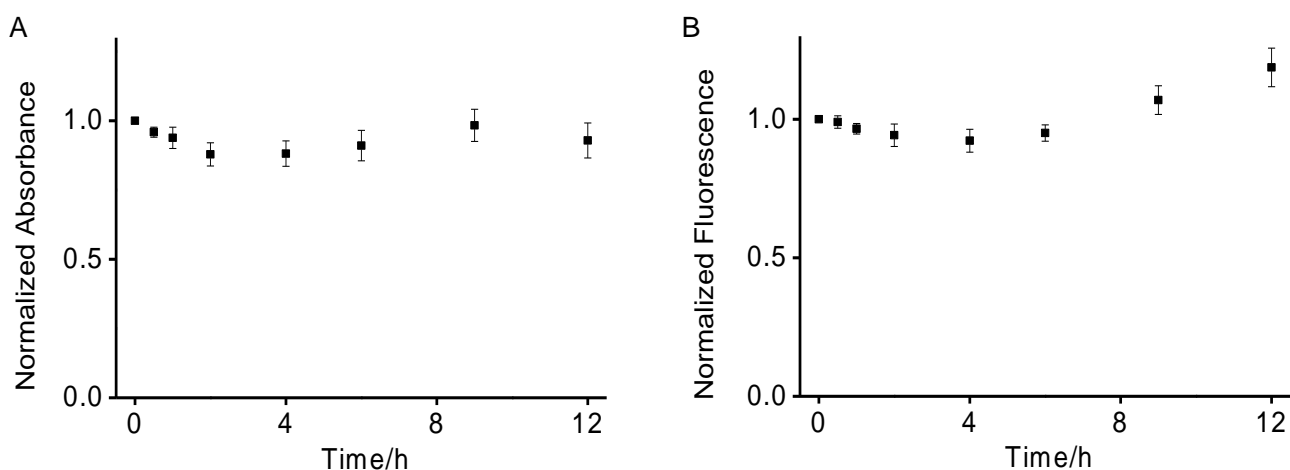


Fig. S13 The stability of RHC-NO₂ (10 μM) at room temperature. Variation of the normalized absorbance at 677 nm (A) and fluorescence intensity at 921 nm (B) of RHC-NO₂ in PBS (pH 7.4) over 12 h. The results are the mean \pm standard deviation of three separate measurements.

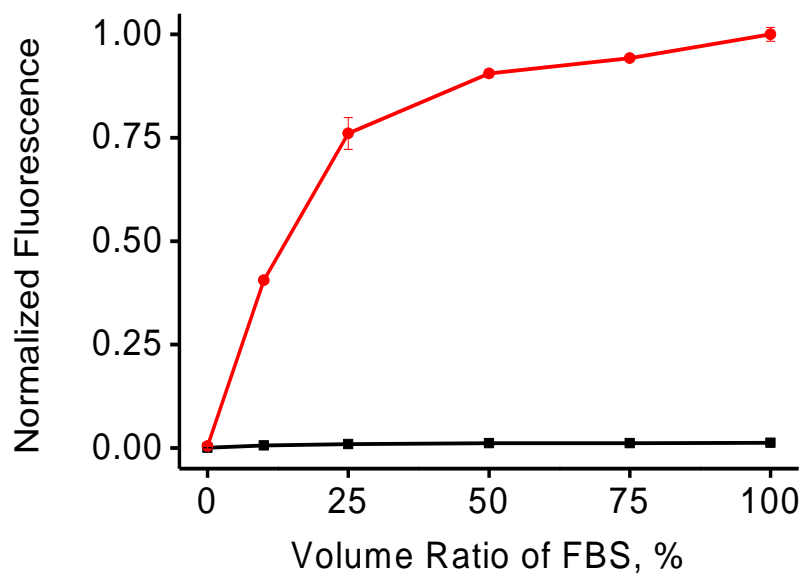


Fig. S14 Normalized fluorescence intensity of 10 μM RHC-NO₂ (black curve) or RHC-NH₂ (red curve) in the phosphate buffer (20 mM, pH 7.4) containing diverse volume fractions of FBS. The results are the mean \pm standard deviation of three separate measurements.

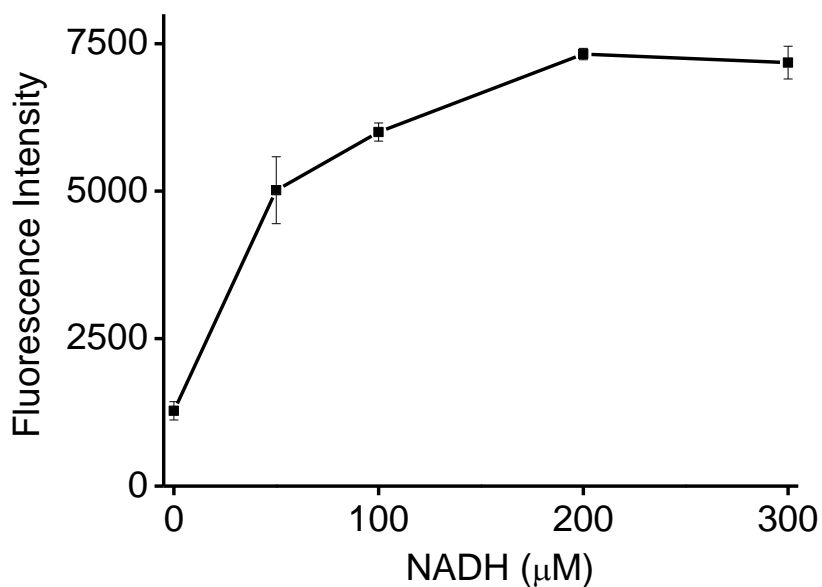


Fig. S15 Fluorescence responses of RHC-NO₂ (10 μM) towards NTR (4 $\mu\text{g}/\text{mL}$) in the presence of different concentrations of NADH. The results are the mean \pm standard deviation of three separate measurements.

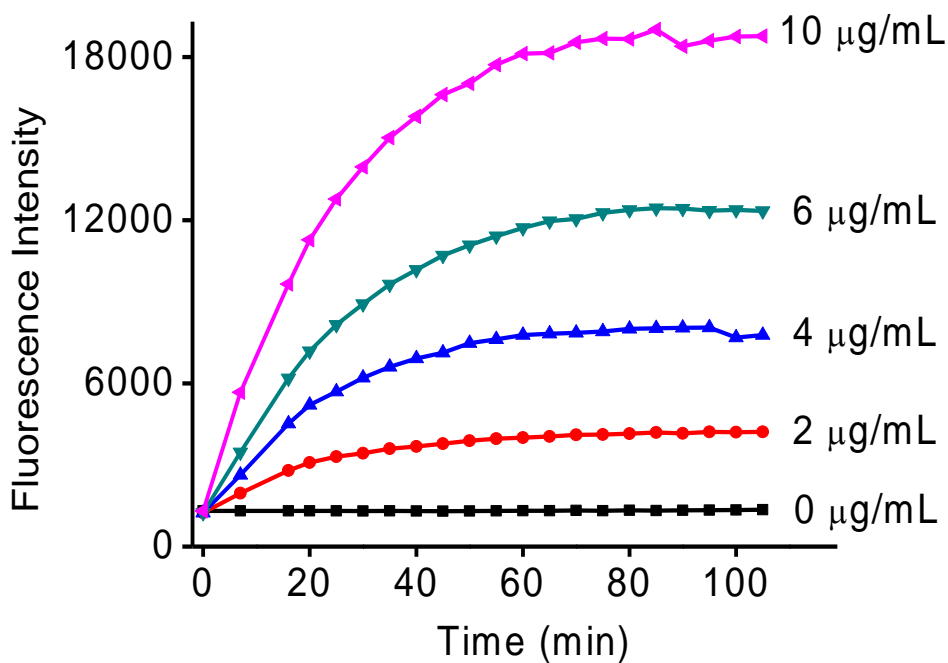


Fig. S16 Effects of reaction time on the fluorescence intensity of RHC-NO₂ (10 μM) with varied concentrations (0, 2, 4, 6 and 10 μg/mL) of NTR. The reactions were performed in the phosphate buffer (pH 7.4, containing 10% FBS) at 37 °C.

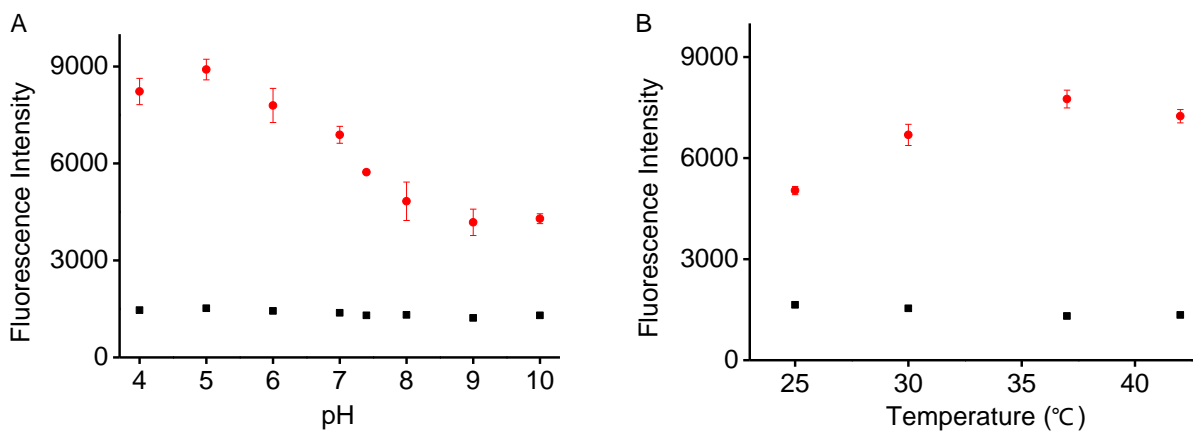


Fig. S17 Effects of pH (A) and temperature (B) on the fluorescence intensity of RHC-NO₂ (10 μM) with (red curve) and without (black curve) NTR (4 μg/mL). The results are the mean ± standard deviation of three separate measurements.

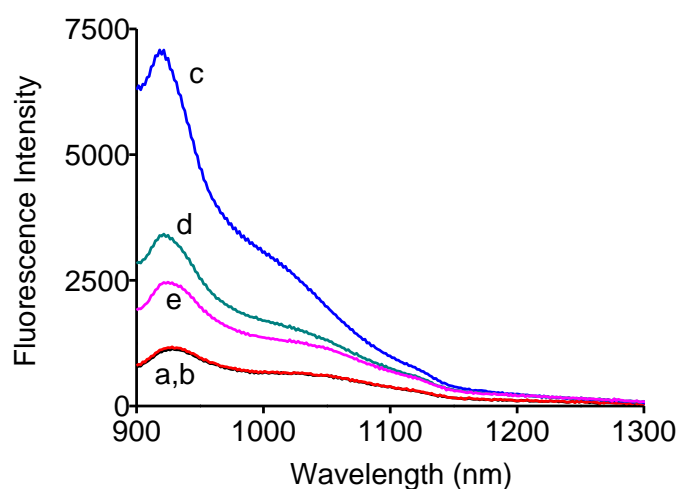


Fig. S18 Fluorescence emission spectra of different reaction systems (excited with 808 nm laser). (a): RHC-NO₂ (10 μM) (control); (b): the system (a) + NADH (200 μM); (c): the system (b) + NTR (4 μg/mL); (d): the system (c) + dicoumarin (0.1 mM); (e): the system (c) + dicoumarin (0.2 mM). Reactions were performed in the phosphate buffer (pH 7.4, containing 10% FBS) at 37 °C for 1 h.

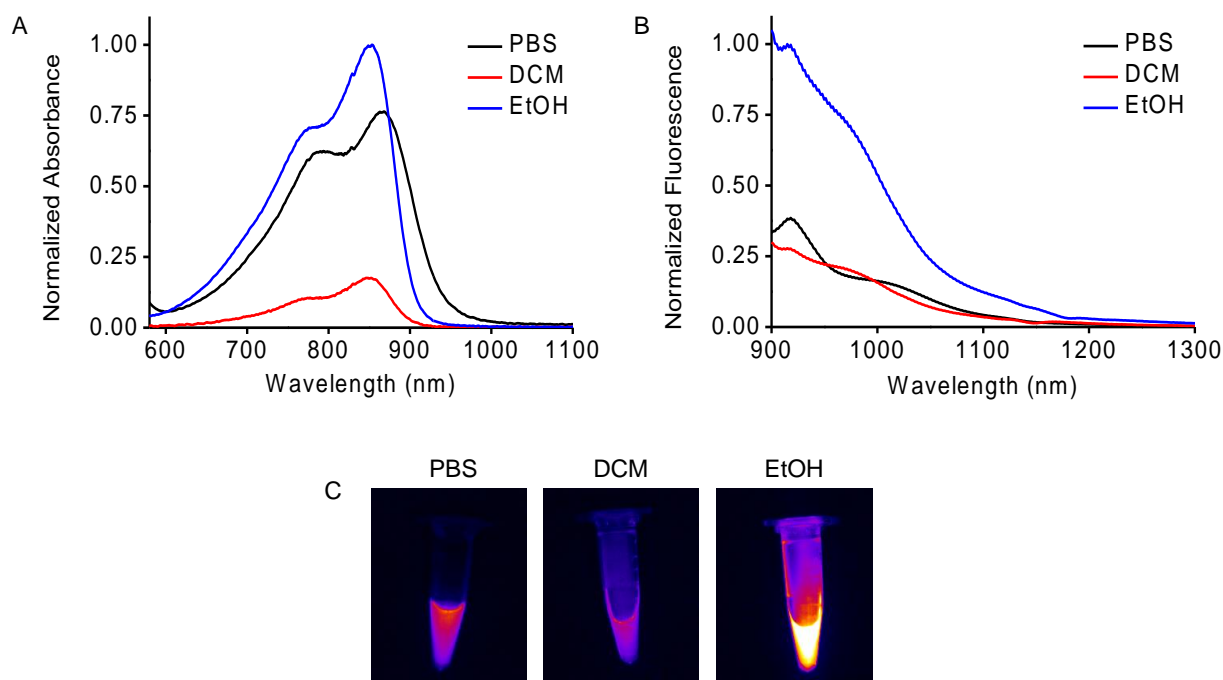
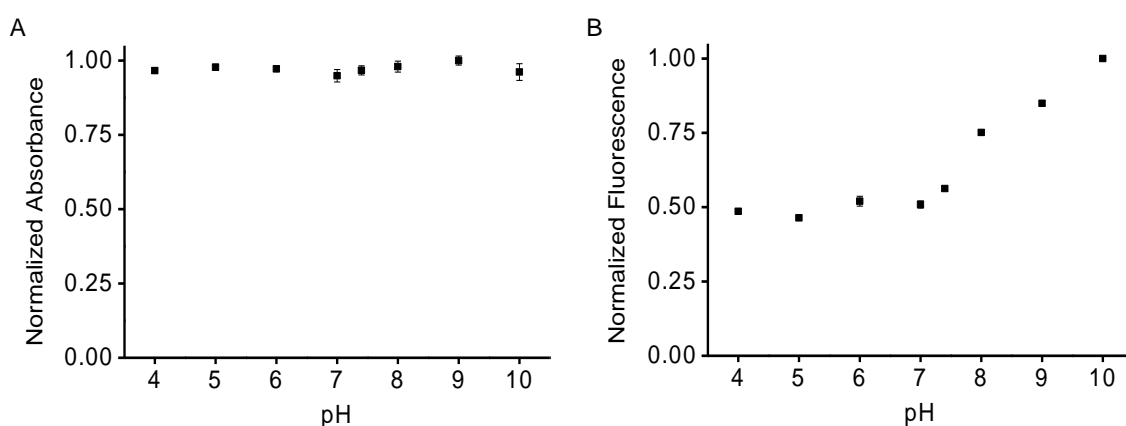
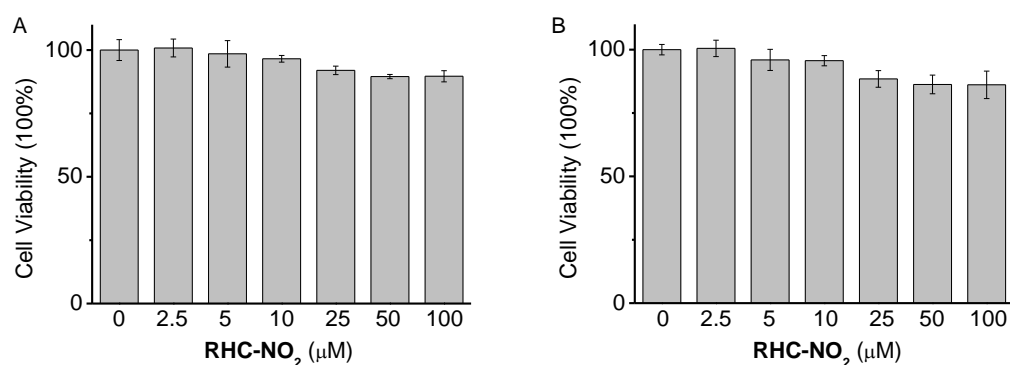


Fig. S19 Spectral properties of RHC-NH₂ (10 μM). Normalized absorption spectra (A) and fluorescence spectra (B) of RHC-NH₂ in PBS (pH 7.4, containing 10% FBS), DCM (dichloromethane) and EtOH, respectively. (C) NIR-II fluorescence images of RHC-NH₂ in different solvents with exposure time of 10 ms using a 1000 nm longpass filter.

Table S1. Photophysical data of RHC-NO₂ and RHC-NH₂ at 25 °C.

Compound	Solvent	λ_{abs} (nm) ^[a]	ϵ (10 ⁴ M ⁻¹ cm ⁻¹) ^[b]	λ_{em} (nm) ^[c]	Φ (%)
RHC-NO ₂	PBS ^[d]	677	1.49	921	<0.01
RHC-NH ₂	DCM	845	0.86	918	0.099
	EtOH	854	4.91	914	0.095
	PBS ^[d]	868	3.75	921	0.124

^[a]Absorption peak. ^[b]Molar absorptivity of the corresponding absorption peak. ^[c]Fluorescence emission peak. ^[d]Measured in the phosphate buffer (pH 7.4, containing 10% FBS).

**Fig. S20** Effects of pH on the absorbance at 868 nm (A) and fluorescence intensity at 921 nm (B) of RHC-NH₂ (10 μM). The results are the mean ± standard deviation of three separate measurements.**Fig. S21** Cell viability changes of (A) A549 and (B) HeLa treated with RHC-NO₂ at different concentrations for 24 h. The results are the mean ± standard deviation of five separate measurements.

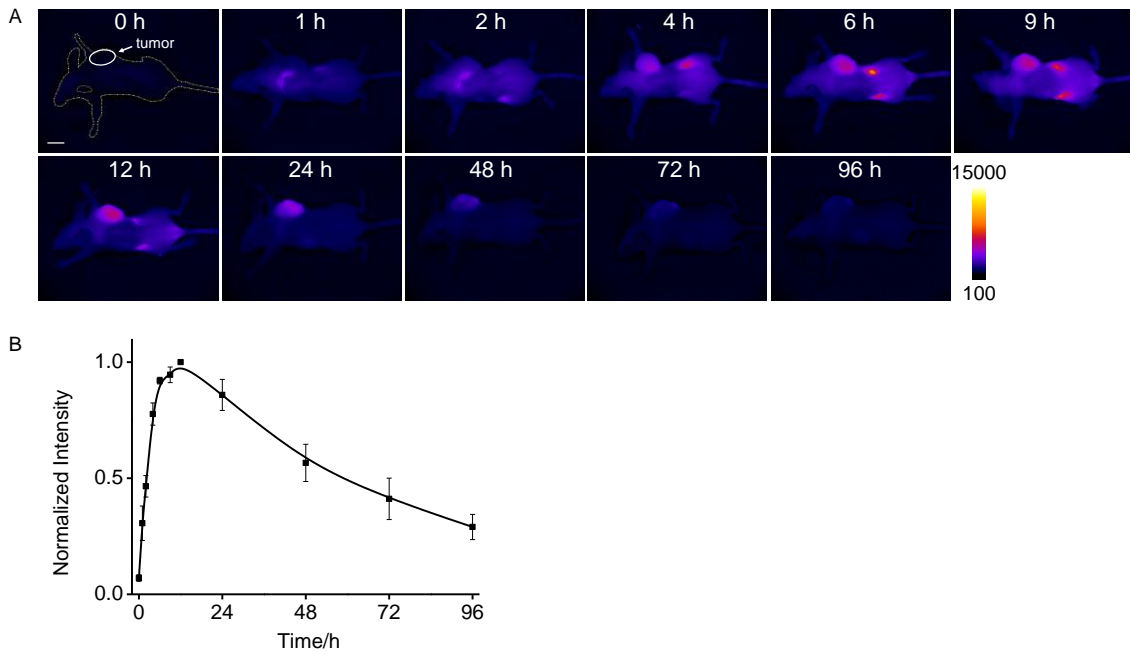


Fig. S22 Representative NIR-II images of A549 tumor-bearing mice ($n = 3$) at different time points after a tail vein injection of RHC-NO₂ (200 μ L, 500 μ M) with 808 nm excitation, 1000 nm longpass filter emission filter and exposure time of 50 ms. Scale bar: 1 cm.

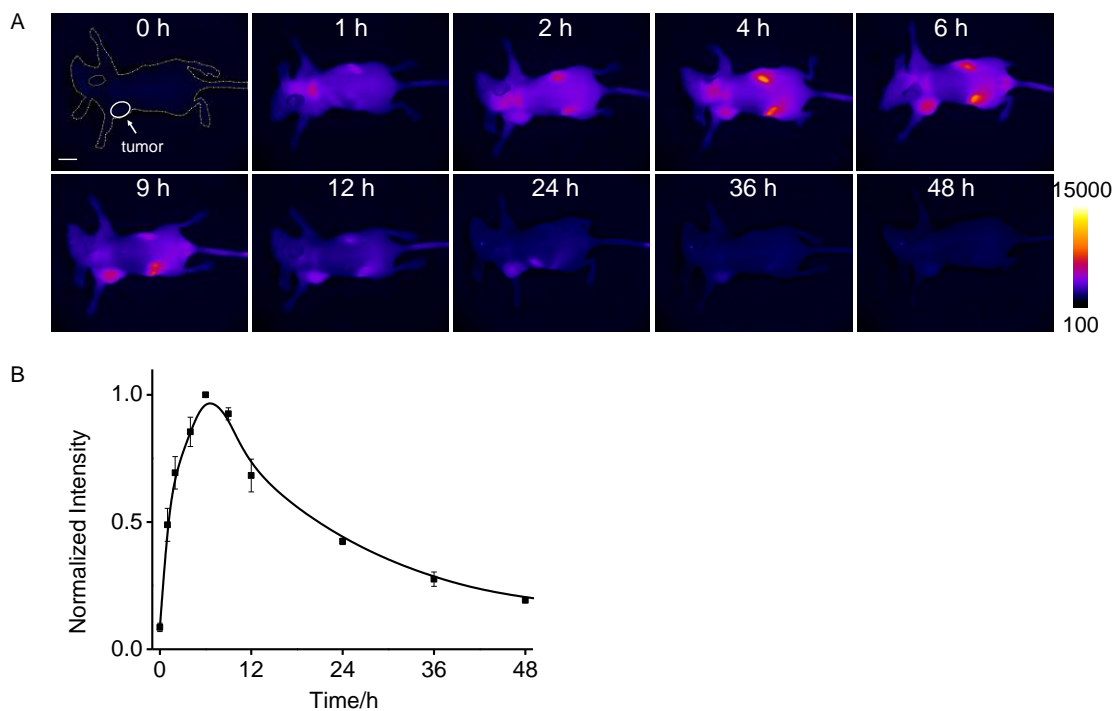


Fig. S23 Representative NIR-II images of HeLa tumor-bearing mice ($n = 3$) at different time points after a tail vein injection of RHC-NO₂ (200 μ L, 500 μ M) with 808 nm excitation, 1000 nm longpass emission filter and exposure time of 50 ms. Scale bar: 1 cm.

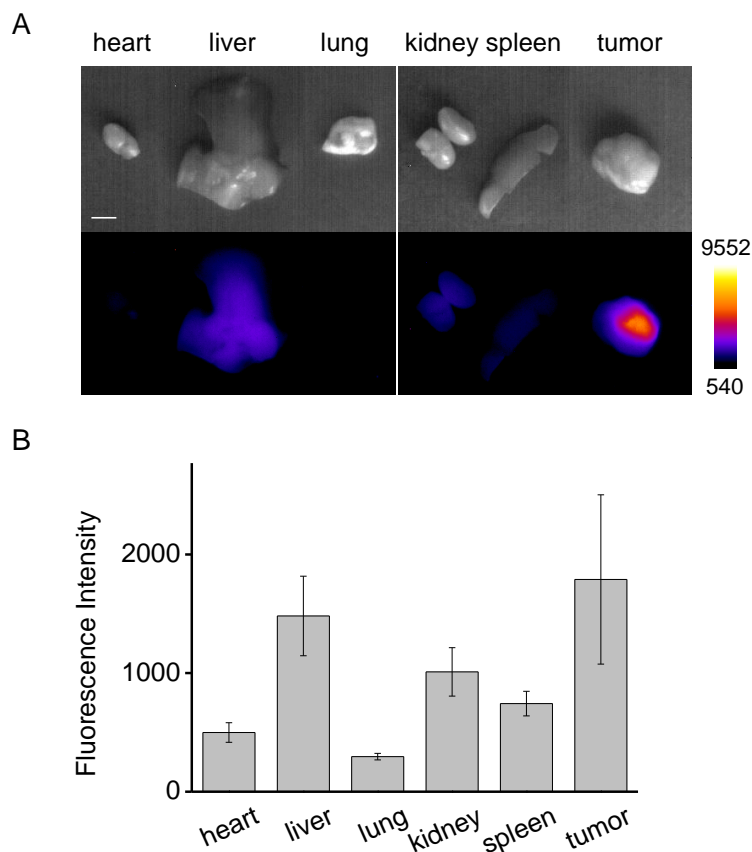


Fig. S24 *Ex vivo* biodistribution of RHC-NO₂ in HeLa tumor-bearing mice after a tail vein injection of RHC-NO₂ (200 μ L, 500 μ M). (A) NIR-II fluorescence imaging of dissected organs and tumor at 48 h post-injection of RHC-NO₂ (with 808 nm excitation, 1000 nm longpass emission filter and exposure time of 50 ms). (B) Quantified fluorescence intensity in HeLa tumor-bearing mice (n = 3). Scale bar: 5 mm.

9. References

1. L. Yuan, W. Lin, Y. Yang and H. Chen, *J. Am. Chem. Soc.*, 2012, **134**, 1200-1211.
2. N. Karton-Lifshin, E. Segal, L. Omer, M. Portnoy, R. Satchi-Fainaro and D. Shabat, *J. Am. Chem. Soc.*, 2011, **133**, 10960-10965.
3. O. E. Semonin, J. C. Johnson, J. M. Luther, A. G. Midgett, A. J. Nozik and M. C. Beard, *J. Phys. Chem. Lett.*, 2010, **1**, 2445-2450.
4. Q. Q. Wan, S. M. Chen, W. Shi, L. H. Li and H. M. Ma, *Angew. Chem. Int. Ed.*, 2014, **53**, 10916-10920.